Simulating superluminal propagation of Dirac particles using trapped ions

Qianqian Chen, Yaoming Chu,[*] and Jianming Cai [†]

School of Physics, Hubei Key Laboratory of Gravitation and Quantum Physics, Institute for Quantum Science and Engineering, International Joint Laboratory on Quantum Sensing and Quantum Metrology, Huazhong University of Science and Technology, Wuhan 430074, China; Wuhan National Laboratory for Optoelectronics, Huazhong University of Science and Technology, Wuhan 430074, China; and State Key Laboratory of Precision Spectroscopy, East China Normal University, Shanghai 200062, China

Simulating quantum phenomena in extreme spacetimes in the laboratory represents a powerful approach to explore fundamental physics in the interplay of quantum mechanics, quantum field theory, and general relativity. Here we propose to simulate the movement of a Dirac particle propagating with a superluminal velocity caused by the emergent Alcubierre warp drive spacetime using trapped ions. We demonstrate that the platform allows for observing the tilted light cone that manifests as a superluminal velocity, which is in agreement with the prediction of general relativity. Furthermore, the *Zitterbewegung* effect arising from relativistic quantum mechanics persists with the superluminal propagation and is experimentally measurable. The present scheme can be extended to simulate the Dirac equation in other exotic curved spacetimes, thus providing a versatile tool to gain insights into the fundamental limit of these extreme spacetimes.

I. INTRODUCTION

Quantum field theory in curved spacetime [1–3], as a semi-classical approach to study the movement of quantized matter fields in a fixed gravitational background, has predicted many striking phenomena such as the famous Hawking radiation and cosmological particle production. However, confirmation of those extremely weak quantum effects in real gravity experiments remains highly unlikely with present technology [4,5]. Following Unruh's pioneering work [6], much attention has turned into sound waves traveling against the classical [7] and quantum fluids [8–19], or light in nonlinear optical platforms [20–23] to effectively emulate quantum field theory in curved spacetime. Remarkably, these relevant analog experiments among many others [24,25] have brought us a better understanding of the relationship between the classical spacetime structure and the quantum theory [26–28].

Furthermore, recent developments of precise and flexible quantum control also facilitate a quantum simulation of related relativistic phenomena [29–40], and the theoretical solutions can thereby be detailed tested. As a representative example, intriguing quantum dynamics related to a Dirac particle moving in curved spacetime has increasingly attracted investigations via the particularly promising trapped-ion platform [41–44]. The exceptional controllability of quantum simulators makes it feasible to emulate a Dirac particle in "exotic" curved spacetimes [43]. As a particularly important example, the Alcubierre warp drive, consistent with the framework of general relativity, can result in faster-than-light propulsion of a spaceship [45]. Compared to the extreme

difficulty in realizing such a time-machine model (i.e., creating warp bubbles) in the actual world [46–48], observation of analog phenomenon with well-controllable quantum simulators in the laboratory should be more accessible. In particular, although the Alcubierre metric is an exact solution to the Einstein field equations, the corresponding matter source violates the energy conditions in classical theory. However, quantum mechanics allows negative energy densities and certain quantum fields violate the energy conditions. The question about the energy conditions remains under debate [49–52]. Interestingly, some kinematical analogs of the superluminal-traveling spacetime do not require the energy conditions [53]. Similarly, quantum simulating exotic spacetime structures may also serve as starting points to shed new light on the energy conditions from the distinctive perspective of quantum mechanics. Besides, merging of fundamental concepts from different fields when implementing such novel quantum simulation, including gravitation, quantum squeezing, and quantum entanglement, would provide a fruitful way to reveal unique features of quantum effects in both the exotic curved spacetimes [43] and the basic light-matter interaction models [42].

In this article, we propose a trapped-ion quantum simulation of a Dirac particle propagating with a superluminal velocity caused by the emergent Alcubierre warp drive spacetime [45] (see Fig. 1). The Hamiltonian from the Dirac equation in the Alcubierre (1+1)-dimensional universe is mapped onto a spin-boson interaction quantum model, which can be further realized by a combination of sideband drives and a periodic modulation of the trapping potential. Remarkably, the tunability of system parameters in the well-controlled trapped-ion platform allows us to access the crossover from flat to curved spacetimes. Using exact numerical simulations, we demonstrate that, in this platform, one is able to observe

―――――――
[*]yaomingchu@hust.edu.cn
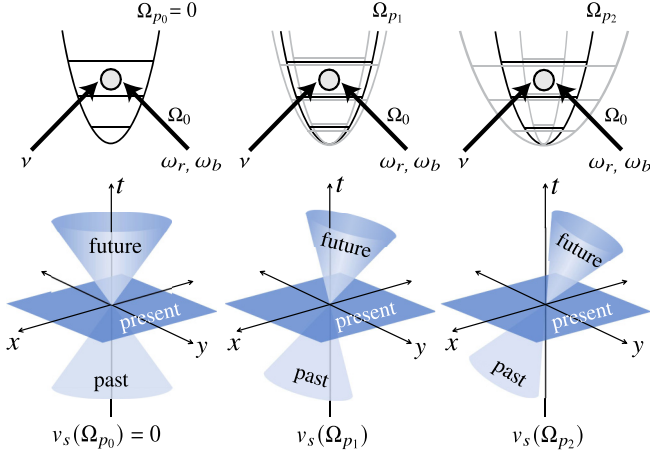[†]jianmingcai@hust.edu.cn

FIG. 1. Schematic illustration of the light cones for Dirac particles in the Alcubierre warp drive spacetime which can be simulated by a trapped-ion system. The key ingredients include (I) the qubit-motion coupling Ω_0 which is implemented by blue and red sideband drives at frequencies ω_b and ω_r, respectively, and (II) the modulation of the confining potential on resonance with the ion-trapping frequency ν, the amplitude of which is given by the parametric coupling strength Ω_p. The tilt of the light cones increases as the parametric coupling strength Ω_p and thereby the Alcubierre metric parameter v_s becomes larger, which results in a superluminal velocity. The tunability of the control parameters within the state-of-the-art experiments makes it feasible to simulate the tilted Dirac equation in the Alcubierre metric in different parameter regions.

some counterintuitive quantum relativistic features such as analog superluminal travel of Dirac particles in the tilted light cones, as well as the *Zitterbewegung* effect of massive Dirac particles incorporating the tilt of the Dirac cone. The present work may pave the way for future research on simulating the Dirac equation in more general exotic curved spacetimes to explore intriguing phenomena arising from the interplay of quantum field theory and general relativity in well-controllable quantum experiments in the laboratory.

II. SIMULATION OF ALCUBIERRE METRIC USING TRAPPED IONS

We start by first introducing the Alcubierre metric [45,54], which is given by

$$ds^2 = c^2 dt^2 - [dx - v_s(t)dt]^2 - dy^2 - dz^2, \quad (1)$$

where $v_s(t) \equiv dx_s(t)/dt$ is the dimensionless velocity value associated with a certain trajectory $x_s(t)$. In the (1+1)-dimensional case, the light cones at a point in the t-x plane are specified by the curves emerging from the point with $ds^2 = 0$, namely

$$\frac{1}{c}\frac{dx}{dt} = v_s(t) \pm 1. \quad (2)$$

If $v_s(t) = 0$, then the spacetime is flat. Otherwise, the corresponding light cones are tipped over and the particle traveling inside the light cone can have a velocity faster than the light speed in the flat spacetime, which is theoretically consistent with the framework of general relativity [45].

Extension of the Dirac equation into curved spacetimes successfully merges quantum mechanics with the general relativity. In the (1+1)-dimensional spacetime with signature $(+, -)$, the Dirac equation reads [41,55]

$$\left[i\hbar\gamma^a e^{\mu}_{(a)}\partial_\mu + \frac{i\hbar}{2}\gamma^a \frac{1}{\sqrt{-g}}\partial_\mu\left(\sqrt{-g}e^{\mu}_{(a)}\right) - mc \right]\psi = 0, \quad (3)$$

where the Greek letter μ and the Latin letter a denote the coordinates of curved spacetime and local rest frame, respectively, m is the mass of the quantized field, g is the determinant of the metric tensor $g^{\mu\nu}$, and $e^{\mu}_{(a)}$ is the vielbein allowing the constant Dirac matrices γ^a to act at each spacetime point. Here, we choose the chiral representation such that $\gamma^0 = \sigma_x$ and $\gamma^1 = -i\sigma_y$, with $\boldsymbol{\sigma}$ the Pauli matrices. In the specific case of the Alcubierre spacetime, the metric tensor is given by

$$g^{\mu\nu} = \begin{pmatrix} 1 - v_s(t)^2 & v_s(t) \\ v_s(t) & -1 \end{pmatrix}, \quad (4)$$

and the vielbein can be set as

$$e^{\mu}_{(a)} = \begin{pmatrix} -1 & 0 \\ -v_s(t) & -1 \end{pmatrix}, \quad (5)$$

with a and μ the column and row indices, respectively. By multiplying Eq. (A1) with σ_z, the Dirac equation can be expanded as

$$\left[-mc^2\sigma_z + i\hbar\sigma_x\frac{\partial}{\partial x} - i\hbar\sigma_y\left(iv_s(t)\frac{\partial}{\partial x} + i\frac{\partial}{\partial(ct)}\right) \right]\psi(t, x) = 0, \quad (6)$$

which can be further rewritten in the form of a Schrödinger equation as follows:

$$i\hbar\partial_t\psi = \left(-ic\hbar v_s(t)\frac{\partial}{\partial x} - ic\hbar\sigma_z\frac{\partial}{\partial x} - mc^2\sigma_x \right)\psi, \quad (7)$$

from which the Hamiltonian H that governs the above dynamical evolution can be written as

$$H = cA\hat{P}\sigma_z + cA\hat{P}v_s(t) - mc^2\sigma_x. \quad (8)$$

Here we introduce the operators $\hat{X}$ and $\hat{P}$

$$\hat{X} \equiv A\hat{x}, \quad \hat{P} \equiv -i\hbar\frac{\partial}{\partial X} \quad (9)$$

to rescale the spatial coordinate x of the simulated Dirac particle by a dimensionless factor A. Note that $\hat{X}$ and $\hat{P}$ will be the observables of the trapped ion in our proposed simulation platform. We remark that the second term of the Hamiltonian in Eq. (8), which is linearly dependent on the momentum $\hat{P}$, is an evidence of relativistic physics [56]. Based on the standard commutation relation $[\hat{X}, \hat{P}] = i\hbar$, the operators $\hat{X}$ and $\hat{P}$ can be further mapped to a bosonic field of frequency ν,

$$\hat{X} = \sqrt{\frac{\hbar}{2m_0\nu}}(\hat{a} + \hat{a}^\dagger), \quad \hat{P} = -i\sqrt{\frac{\hbar m_0\nu}{2}}(\hat{a} - \hat{a}^\dagger), \quad (10)$$

where m_0 is a constant with the dimension of mass.

By substituting Eq. (A7) into Eq. (8) and applying the Hadamard transformation (i.e., $\sigma_x \to \sigma_z$, $\sigma_z \to \sigma_x$), the Hamiltonian can be rewritten as

$$H = -icA\sqrt{\frac{\hbar m_0\nu}{2}}(\hat{a} - \hat{a}^\dagger)[\sigma_x + v_s(t)] - mc^2\sigma_z. \quad (11)$$

To simulate the above Hamiltonian in Eq. (11) with the tunable parameter v_s, we consider a setup of a single ion trapped above a linear surface electrode radio-frequency trap. The radial motional mode of the trapped ion with a frequency ν models a harmonic oscillator and its two internal ground hyperfine levels with the transition frequency ω_0 playing the role of an effective spin 1/2, denoted as $|\uparrow\rangle$ and $|\downarrow\rangle$. As an example, the present scheme may employ a trapped $^{25}\mathrm{Mg}^+$ ion hyperfine qubit, with an out-of-phase radial motional mode frequency $\nu \approx 2\pi \times 5.9$ MHz [57]. The qubit states are chosen as $|\downarrow\rangle \equiv |F = 3, m_F = 1\rangle$ and $|\uparrow\rangle \equiv |F = 2, m_F = 1\rangle$ [57,58], where F is the total angular momentum and m_F is its projection along the quantization axis.

The spin-harmonic-oscillator coupling of the form in Eq. (11) can be realized by implementing the Mølmer–Sørensen interaction [59]

$$H_{\Omega_0} = \hbar\Omega_0\{|\uparrow\rangle\langle\downarrow| \otimes [\hat{a}^\dagger \sin(\omega_b t) - \hat{a} \sin(\omega_r t)] + \mathrm{H.c.}\}$$

(12)

via simultaneous blue and red sideband driving at frequencies ω_b and ω_r, respectively, which in real experiments can be generated by using oscillating near-field magnetic-field gradients [60]. Here, the frequencies of the blue and red sideband drives satisfy the condition $\omega_b - \nu = \omega_r + \nu = \omega_0 - \Delta$. In addition, we introduce a periodic modulation of the single ion's trapping potential of the strength $\Omega_p(t)$ at frequency ν to obtain the second term $\sim cv_s(t)\hat{P}$ in Eq. (11). The corresponding Hamiltonian is given by

$$H_{\Omega_p} = \hbar\Omega_p(t) \sin(\nu t)(\hat{a} + \hat{a}^\dagger)^2.$$

(13)

This can be experimentally implemented by applying an oscillating potential directly to the radio-frequency trapping electrodes, as demonstrated in Ref. [57]. Therefore, such a trapped-ion platform can be characterized by the following system Hamiltonian as

$$H_{\mathrm{ion}} = \frac{\hbar\omega_0}{2}\sigma_z + \hbar\nu\hat{a}^\dagger\hat{a} + H_{\Omega_p} + H_{\Omega_0}.$$

(14)

By making a displacement transformation $a \to a + \eta$ and $a^\dagger \to a^\dagger + \eta$ ($\eta \ll 1$) with the operator $\mathcal{D}[\eta] = e^{\eta(a^\dagger - a)}$, and then moving to the interaction picture with respect to $H_0 = \hbar(\omega_0 - \Delta)/2\sigma_z + \hbar\nu a^\dagger a$, the effective Hamiltonian can be approximated as

$$H_I(t) \simeq \frac{\hbar\Delta}{2}\sigma_z - 2i\hbar\eta\Omega_p(t)(\hat{a} - \hat{a}^\dagger) + \frac{\hbar\Omega_0}{2i}(\hat{a} - \hat{a}^\dagger)\sigma_x \quad (15)$$

under the conditions of $\{|\Delta|, |\Omega_p(t)|, |\Omega_0|\} \ll \nu \ll \omega_0$. Therefore, it can be seen that the Hamiltonian in Eq. (15) as implemented in the trapped-ion platform is equivalent to the Hamiltonian in Eq. (11) that governs the Dirac equation in the Alcubierre (1+1)-dimensional universe with the parameter correspondence as $v_s(t) \leftrightarrow 4\eta\Omega_p(t)/\Omega_0$, $c \leftrightarrow (\hbar/2m_0\nu)^{1/2}\Omega_0/A$, and $m \leftrightarrow -\hbar\Delta/2c^2$.

We remark that the experimental tunability of the parameters $\{\Omega_0, \Omega_p, \Delta\}$ in the well-controllable trap-ion platform allows access to the crossover from flat to curved spacetimes, namely the tilt of the Dirac equation can be tuned by choosing appropriate values of the parameter Ω_p; see Fig. 1. The angle of the simulated light cone is given by $\theta = \arctan(v_s +$

1) $- \arctan(v_s - 1)$, which decreases for a larger value of v_s, i.e., the velocity of the Dirac particle would be constrained in a smaller range. In the limit case of extremely large v_s, $\arctan(v_s \pm 1) \to \pi/2$, and the angle of the light cone $\theta \to 0$, the trajectory of the trapped ion can be seen as a counterpart of the closed timelike curves.

III. OBSERVATION OF ANALOG SUPERLUMINAL TRAVEL

To show the effective velocity of the simulated Dirac particle, we solve the following Heisenberg equation of the trapped ion system (see Appendix B):

$$\frac{d\hat{x}(t)}{dt} = i[H(t), \hat{x}(t)] = c[v_s(t) + \hat{\phi}_z(t)],$$

(16)

where $\hat{x}(t) = U^\dagger(t)\hat{x}U(t)$ represents the position operator of the Dirac particle and $\hat{\phi}_z(t) = U^\dagger(t)\sigma_z U(t)$ with $U(t)$ the evolution operator from the Hamiltonian $H(t)$ in Eq. (8). We remark that Eq. (16) is consistent with the Alcubierre metric, since the two eigenvalues ± 1 of $\hat{\phi}_z(t)$ correspond to the two opposite directions of the velocity. The mechanical degrees of freedom of the trapped ion $\hat{X}$ is related to the spatial coordinate of the simulated Dirac particle $\hat{x}$ by $\hat{X} \equiv A\hat{x}$ [see Eq. (9)]; thus the velocity $d\langle\hat{X}\rangle/dt$ is in the range of $Ac(v_s \pm 1)$.

As an illustrative example, we choose the initial state of the trapped ion as $|\psi_0\rangle = \mathcal{N}\pi^{-1/4}\int dX \exp(-X^2/2)|X\rangle \otimes |s\rangle$, where $|X\rangle$ and $|s\rangle$ represent the spatial and internal degrees of freedom of the trapped ion, respectively. Without loss of generality, the spatial wave function satisfies a Gaussian distribution with $\mathcal{N}$ the normalization factor. In Figs. 2(a) and 2(b), we show the trajectory $\langle\hat{x}(t)\rangle$ (in the unit of c) of the simulated massless Dirac particle (i.e., $m = 0$) as a function of the evolution time. According to Eq. (16), the trajectory of the evolving states from the initial spin states $|\uparrow\rangle$ and $|\downarrow\rangle$ (namely the two eigenstates of $\langle\sigma_z\rangle = \pm 1$) specifies the shape of the simulated light cone. It can be seen that, corresponding to massless Dirac particles, the light cones for different values of the parameter v_s are consistent with the analytical results from classical general relativity theory [43]. In particular, the simulated light cones start to tip over as the parameter v_s increases, which indicates that the spacetime becomes more curved. These numerical simulation results demonstrate that the quantum simulation using trapped ions can confirm the superluminal propagation of Dirac particles in the Alcubierre warp drive spacetime.

In the cases of initial states with $|s\rangle = |\uparrow\rangle$ or $|\downarrow\rangle$, the velocity is well defined, and thus the wave packet of the simulated Dirac particle remains localized, as shown by the blue line and green circles in Fig. 2(c). In contrast, if we start from a coherent superposition state $|s\rangle = (|0\rangle + |1\rangle)/\sqrt{2}$, the wave packet of the simulated Dirac particle has two peaks which correspond to the initial velocities $c(v_s \pm 1)$, respectively, resulting in an increase of the variance of the trajectory; see the orange line in Fig. 2(c).

IV. *ZITTERBEWEGUNG* EFFECT WITH SUPERLUMINAL PROPAGATION

In addition to the analog superluminal propagation, we also find that, for massive Dirac particles with $m \neq 0$, the
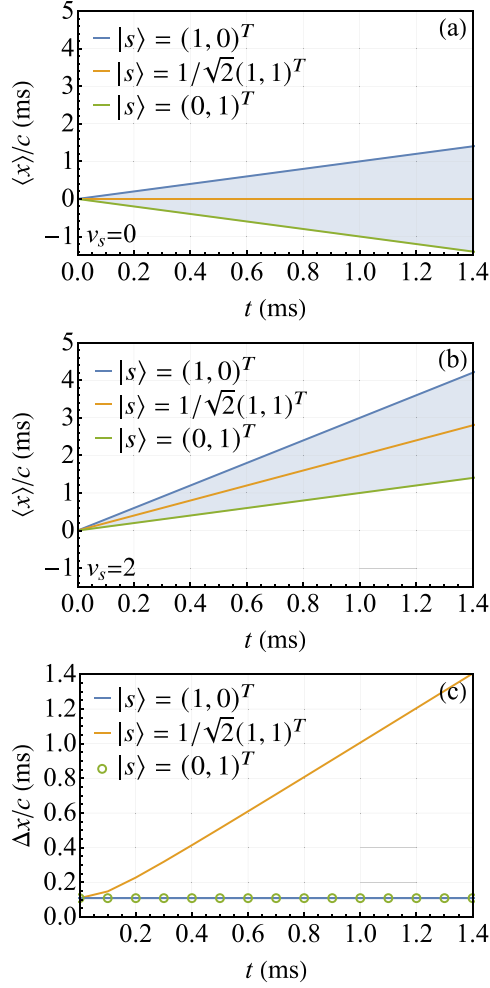
FIG. 2. Dynamics of a trapped-ion simulated massless ($m = 0$) Dirac particle in the Alcubierre space-time. (a), (b) The light cones of the simulated Dirac particle (blue shaded) are illustrated by its coordinate $\langle \hat{x} \rangle$, which is obtained from the average position of the trapped ion as $\langle \hat{x} \rangle = \langle \hat{X} \rangle / A$ for the Alcubierre metrics with (a) $v_s = 0$ (flat space-time) and (b) $v_s = 2$ (curved space-time). (c) The variance of the simulated Dirac particle's position Δx as a function of the evolution time for $v_s = 2$. In (a)–(c), the initial state of the trapped ion is chosen as $|\psi_0\rangle \sim \mathcal{N} \pi^{-1/4} \int dX \, \exp(-X^2/2)|X\rangle \otimes |s\rangle$, where $|X\rangle$ and $|s\rangle$ denote the spatial and internal degrees of freedom of the trapped ion. The internal states are chosen as $|s\rangle = (1, 0)^T$ [blue, or the upper boundary of the shaded regions in (a), (b) and the flat line in (c)], $|s\rangle = (0, 1)^T$ [green, or the lower boundary of the shaded regions in (a), (b) and the circles in (c)], and $|s\rangle = 1/\sqrt{2}(1, 1)^T$ [orange, or the middle lines in the shaded regions in (a), (b) and the increasing line in (c)]. The parameters used in numerical calculations are $\Omega_0 = 2\pi \times 1.46$ kHz, $\Omega_p = 2\pi \times 50$ kHz, $\nu = 2\pi \times 5.9$ MHz, and $\Delta = 0$.

Zitterbewegung effect induces an oscillatory behavior in the trajectory of the trapped ion. This effect is caused by the quantum superpositions of electron and positron solutions of the free wave packets [44,56] and may exist in both flat and curved spacetime [42,56]. The equation of motion for the expectation value of the position operator $\hat{x}(t)$ in this case can

be obtained as (see Appendix B)

$$\frac{d^2}{dt^2} \langle \hat{x}(t) \rangle = -\frac{2mc^3}{\hbar} \langle e^{2iH_{\text{flat}}t/\hbar} \sigma_y \rangle, \qquad (17)$$

where $H_{\text{flat}} = Ac\hat{P}\sigma_z - mc^2\sigma_x$ represents the Dirac Hamiltonian in the flat spacetime. From Eq. (17), one can see that the oscillatory behavior is induced by the mass m but independent of the parameter v_s and therefore the *Zitterbewegung* effect would persist with the superluminal propagation. In Fig. 3(a), we show that the *Zitterbewegung* effect can manifest for both constant and time-dependent v_s in the trapped-ion simulator. As an example, we consider a time-dependent spacetime by choosing v_s such that both the initial and final velocities are subluminal, which is derived from a trajectory $x_s(t)$ of the simulated Dirac particle. This result is shown by the gray dashed line in Fig. 3(a), which clearly exhibits the *Zitterbewegung* effect.

In Figs. 3(b) and 3(c), we present the properties of the wave packet of the simulated Dirac particle during its evolution. As shown in Fig. 3(b), we do not observe any squeezing of the density profile caused by the simulated gravity in the trapped-ion system, which represents a different phenomenon from the one in Ref. [42]. We remark that the qualitative behavior of the variance of the position is determined by the mass m and is independent of the parameter v_s. The wave packets at $t = 0.3$ ms and $t = 1.5$ ms are shown in Fig. 3(c), which suggests that the wave packet of the simulated Dirac particle is stretched and the oscillatory feature becomes more prominent as the system evolves, due to the *Zitterbewegung* effect.

V. CONCLUSION

To summarize, we propose a scheme to implement a trapped-ion quantum simulation of a Dirac particle moving in the Alcubierre (1+1)-dimensional universe, which is a particularly important example of extremely curved spacetime leading to superluminal propagation consistent with general relativity. We show that the flexibility of control parameters in such a platform allows one to observe counterintuitive effects, including the superluminal velocity and the *Zitterbewegung* effect of the simulated Dirac particle in the Alcubierre curved spacetime. Our work demonstrates the feasibility to explore interesting and counterintuitive features of exotic curved spacetime by quantum simulation of Dirac particles in the corresponding spacetime geometry. Furthermore, the analogy between particles in the setting of semiclassical quantum field theory and basic light-matter interaction quantum models would further inspire the ideas to investigate intriguing phenomena of general relativity and quantum field theory in a variety of quantum platforms that are available in laboratories. Besides, our results may serve as the first step towards experiments to shed new light on the energy condition with the probe of quantum-mechanics experiments, facilitating the understanding of the exotic matters that are responsible for the exotic spacetime geometry. It would also be interesting to investigate novel phenomena in laboratories that are inspired and interpreted by the emergent exotic spacetime structures [61–67] and to discover more materials and phenomena in this family.
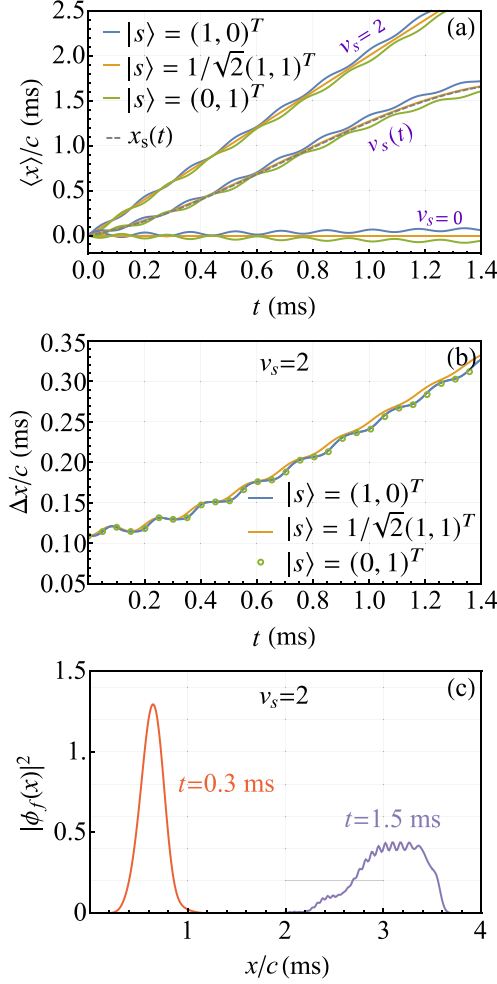
FIG. 3. Observing *Zitterbewegung* effect with superluminal propagation for a trapped-ion simulated massive Dirac particle ($m \neq 0$) in the Alcubierre spacetime. (a) The trajectories of the simulated Dirac particle with different initial internal states for $v_s = 0$ (flat spacetime), $v_s = 2$ (curved spacetime), and $v_s(t) = \partial_t x_s(t)$ where $x_s(t) = 0.56t + 1346t^2 - 642377t^3$. (b) The variance of the simulated Dirac particle's position as a function of the evolution time t for $v_s = 2$. In (a), (b), the internal states are chosen as $|s\rangle = (1, 0)^T$ [blue, or the upper boundary of the sets of lines in (a) and the line overlapping with circles in (b)], $|s\rangle = (0, 1)^T$ [green, or the lower boundary of the sets of lines in (a) and the circles in (b)], and $|s\rangle = 1/\sqrt{2}(1, 1)^T$ [orange, or the middle lines in the sets of lines in (a) and the separate line not overlapping with circles in (b)]. (c) The wave packets of the trapped ion at $t = 0.3$ ms and $t = 1.5$ ms as a function of the coordinate x (in the unit of c). In (a)–(c), the parameters used in numerical calculations are $\Omega_0 = 2\pi \times 1.46$ kHz, $\nu = 2\pi \times 5.9$ MHz, and $\Delta = -2\pi \times 6.1$ kHz.

ACKNOWLEDGMENTS

APPENDIX A: DERIVATION OF THE HAMILTONIAN OF A TRAPPED-ION SIMULATED DIRAC PARTICLE

In the main text, we propose to simulate a Dirac particle moving in the (1+1)-dimensional Alcubierre spacetime with a well-controlled trap-ion quantum simulator. In a semiclassical way, the Dirac particle moving in a fixed gravitational background, characterized by a general metric tensor $g_{\mu\nu}$, can be expressed as [41,55]

$$\left[i\hbar\gamma^a e^\mu_{(a)}\partial_\mu + \frac{i\hbar}{2}\gamma^a \frac{1}{\sqrt{-g}}\partial_\mu\left(\sqrt{-g}e^\mu_{(a)}\right) - mc^2 \right]\psi = 0, \tag{A1}$$

where the Greek letter μ and the Latin letter a denote the coordinates of curved spacetime and local rest frame, respectively, m is the mass of the quantized field, g is the determinant of the metric tensor, and $e^\mu_{(a)}$ is the vielbein allowing the constant Dirac matrices γ^a to act at each spacetime point. Here, we choose the chiral representation such that $\gamma^0 = \sigma_x$, $\gamma^1 = -i\sigma_y$, with $\boldsymbol{\sigma}$ the Pauli matrices. In the specific case of the Alcubierre spacetime, the metric tensor of which is given by

$$g^{\mu\nu} = \begin{pmatrix} 1 - v_s^2 & v_s \\ v_s & -1 \end{pmatrix}, \tag{A2}$$

the vielbein can be set as

$$e^\mu_{(a)} = \begin{pmatrix} -1 & 0 \\ -v_s(t) & -1 \end{pmatrix}, \tag{A3}$$

with a and μ the column and row indices, respectively. By multiplying Eq. (A1) with σ_z, the Dirac equation can be expanded as

$$\left[-mc^2\sigma_z + i\hbar\sigma_x\frac{\partial}{\partial x} - i\hbar\sigma_y\left(iv_s(t)\frac{\partial}{\partial x} + i\frac{\partial}{\partial(ct)} \right) \right]\psi(t, x) = 0, \tag{A4}$$

which can be further rewritten in the form of a Schrödinger equation [i.e., Eq. (7) in the main text] as follows:

$$i\hbar\partial_t\psi(t, x) = \left(-ic\hbar v_s(t)\frac{\partial}{\partial x} - ic\hbar\sigma_z\frac{\partial}{\partial x} - mc^2\sigma_x \right)\psi(t, x). \tag{A5}$$

Thus the Hamiltonian of the Dirac particle to be simulated can be written as

$$H(t) = cA[v_s(t) + \sigma_z]\hat{P} - mc^2\sigma_x, \tag{A6}$$

with $\hat{P} \equiv -i\hbar\partial/\partial\hat{X}$ and $\hat{X} \equiv A\hat{x}$. We remark that the operators $\hat{X}$ and $\hat{P}$, which satisfy the standard commutation relation, i.e., $[\hat{X}, \hat{P}] = i\hbar$, can be related to the position and momentum operators of the trapped ion used to simulate the relativistic Dirac particle. Thereby, we can rewrite them using the creation and annihilation operators as

$$\hat{X} = \sqrt{\frac{\hbar}{2m_0\nu}}(\hat{a} + \hat{a}^\dagger), \quad \hat{P} = -i\sqrt{\frac{m_0\nu}{2\hbar}}(\hat{a} - \hat{a}^\dagger), \tag{A7}$$

with m_0 the mass and ν the trapping potential of the trapped ion. In this way, the Hamiltonian of the trapped-ion simulated Dirac particle can be expressed as

$$H(t) = \frac{cA\hbar}{i\sqrt{2}}(a - a^\dagger)\sigma_z + \frac{cAv_s(t)\hbar}{i\sqrt{2}}(a - a^\dagger) - mc^2\sigma_x, \tag{A8}$$

which is equivalent to Eq. (11) in the main text by considering the Hadamard transformation.

APPENDIX B: QUANTUM DYNAMICS OF THE TRAPPED-ION SIMULATED DIRAC PARTICLE

In this section, we derive the quantum dynamics of the simulated Dirac particle in more detail. Based on the Heisenberg equation, the time evolution of the position and spin operators is given by

$$
\begin{aligned}
\frac{d\hat{x}(t)}{dt} &= \frac{i}{\hbar}[\tilde{H}(t), \hat{x}(t)] = c(v_s(t) + \hat{\phi}_z(t)), \\
\frac{d\hat{\phi}_z(t)}{dt} &= -\frac{2mc^2}{\hbar}\hat{\phi}_y(t),
\end{aligned}
\tag{B1}
$$

where

$$
\hat{x}(t) = U^\dagger(t)\hat{x}U(t), \quad \hat{\phi}_\alpha(t) = U^\dagger(t)\sigma_\alpha U(t), \tag{B2}
$$

with $\alpha = x, y, z$. The effective Hamiltonian and the evolution operator are

$$
\tilde{H}(t) = U^\dagger(t)H(t)U(t), \quad U(t) = \exp\left[-i\int_0^t H(\tau)d\tau/\hbar\right], \tag{B3}
$$

with $H(t) = cA[v_s(t) + \sigma_z]\hat{P} - mc^2\sigma_x$. In the above derivation, we have omitted the time-ordering operator in $U(t)$ due to the fact that $[H(t), H(t')] = 0$ for arbitrary t and t'. From the above equations, we can obtain

$$
\frac{d^2\hat{x}(t)}{dt^2} = \frac{i}{\hbar}[H(t), c\hat{\phi}_z(t)] = -\frac{2mc^3}{\hbar}\hat{\phi}_y(t). \tag{B4}
$$

In order to derive $\hat{\phi}_y(t)$, we notice that $\{\sigma_y, H(t)\} = 2Acv_s(t)\hat{P}\sigma_y$, which gives $\sigma_y H(t)\sigma_y = -H(t) + 2Acv_s(t)\hat{P}$ and further

$$
\begin{aligned}
\hat{\phi}_y(t) &= \exp\left(i\int H(t)dt/\hbar\right)\sigma_y\exp\left(-i\int H(t)dt/\hbar\right) \\
&= \exp\left(i\int H(t)dt/\hbar\right)\exp\left(-i\int \sigma_y H(t)\sigma_y dt/\hbar\right)\sigma_y \\
&= \exp\left[2i\int\left(H(t) - Acv_s(t)\hat{P}\right)dt\right]\sigma_y \\
&\equiv \exp\left(2iH_{\text{flat}}t/\hbar\right)\sigma_y,
\end{aligned}
\tag{B5}
$$

where $H_{\text{flat}} = Ac\hat{P}\sigma_z - mc^2\sigma_x$ corresponds to the Dirac Hamiltonian in the flat spacetime. Hence we have [i.e., Eq. (17) in the main text]

$$
\frac{d^2\langle\hat{x}(t)\rangle}{dt^2} = -\frac{2mc^3}{\hbar}\langle e^{2iH_{\text{flat}}t/\hbar}\sigma_y\rangle. \tag{B6}
$$

APPENDIX C: TRAPPED-ION REALIZATION OF THE DIRAC HAMILTONIAN

The well-controllable trapped-ion system is a particularly promising platform for simulating the basic light-matter interaction models by exploiting its internal and motional degrees of freedom. Here we explain in more detail the trapped-ion setup to simulate the Dirac particle moving in curved spacetime, the Hamiltonian of which [i.e., Eq. (11) in the main text]

has been derived in the above section. We consider the radial motional mode with frequency v of the trapped ion to model the bosonic field and the two internal ground hyperfine levels with transition frequency ω_0 to form an effective spin $1/2$, denoted as $|\uparrow\rangle$ and $|\downarrow\rangle$. With blue and red sideband drives at frequencies ω_b and ω_r, respectively [57,59], which can be generated by using oscillating near-field magnetic-field gradients in experiments [60], one is able to realize the spin-harmonic-oscillator coupling via the Mølmer–Sørensen interaction that is described as

$$
H_{\Omega_0} = \hbar\Omega_0\{|\uparrow\rangle\langle\downarrow| \otimes [a^\dagger\sin(\omega_b t) - a\sin(\omega_r t)] + \text{H.c.}\}. \tag{C1}
$$

In addition, it is possible to apply an oscillating potential directly to the radio-frequency trapping electrodes such that the single ion's trapping potential is modulated periodically with an amplitude $\Omega_p(t)$ at frequency v. The corresponding Hamiltonian is given by

$$
H_{\Omega_p} = \hbar\Omega_p(t)\sin(vt)(a + a^\dagger)^2. \tag{C2}
$$

Therefore, the total Hamiltonian of such a trapped-ion setup is [namely Eq. (C3) in the main text]

$$
H_{\text{ion}} = \frac{\hbar\omega_0}{2}\sigma_z + \hbar v a^\dagger a + H_{\Omega_p} + H_{\Omega_0}. \tag{C3}
$$

In order to derive the Hamiltonian of Eq. (11) in the main text, we first make a displace transformation to the above Hamiltonian with $\mathcal{D}[\eta] = e^{\eta(a^\dagger - a)}$, $\eta \ll 1$, which gives

$$
\begin{aligned}
H'_{\text{ion}} &= \mathcal{D}^\dagger[\eta]H_{\text{ion}}\mathcal{D}[\eta] \\
&= \frac{\hbar\omega_0}{2}\sigma_z + \hbar v a^\dagger a + \hbar v\eta(a + a^\dagger) \\
&\quad + \hbar\Omega_0\{|\uparrow\rangle\langle\downarrow|[(a^\dagger + \eta)\sin(\omega_b t) - (a + \eta)\sin(\omega_r t)] + \text{H.c.}\} \\
&\quad + \frac{\hbar\Omega_p}{2i}(e^{ivt} - e^{-ivt})[a^2 + a^{\dagger 2} + aa^\dagger + a^\dagger a \\
&\quad + 4\eta(a + a^\dagger) + 4\eta^2].
\end{aligned}
\tag{C4}
$$

Then we move to the interaction picture with respect to $H_0 = \hbar(\omega_0 - \Delta)/2\sigma_z + \hbar v a^\dagger a$ while requiring $\omega_b - v = \omega_r + v = \omega_0 - \Delta$. After applying the rotating-wave approximation under the conditions of $\{|\Delta|, |\Omega_p(t)|, |\Omega_0|\} \ll v \ll \omega_0$, we are left with

$$
\begin{aligned}
H_{I,\text{ion}} &\simeq \frac{\hbar\Delta}{2}\sigma_z + \frac{\hbar\Omega_0}{2i}[|\uparrow\rangle\langle\downarrow|(a - a^\dagger) + \text{H.c.}] \\
&\quad - 2i\eta\hbar\Omega_p(a - a^\dagger),
\end{aligned}
\tag{C5}
$$

the form of which is equivalent to the Hamiltonian of Eq. (15) in the main text by further making the Hadamard transformation.

APPENDIX D: NUMERICAL SIMULATION OF THE TRAPPED-ION SIMULATED DIRAC PARTICLE

Without loss of generality, the initial state of the trapped ion is chosen as

$$
|\psi_0\rangle = \mathcal{N}\pi^{-1/4}\int dX \exp(-X^2/2)|X\rangle|s\rangle, \tag{D1}
$$

where $|X\rangle$ and $|s\rangle$ denote the spatial and internal degrees of freedom of the trapped ion, respectively, and $\mathcal{N}$ is the

normalization factor of its wave function. Using the following relation:

$$\langle X|n\rangle = (\sqrt{2}/2)^n (n!)^{-1/2} \pi^{-1/4} e^{-X^2/2} H_n(X), \qquad \text{(D2)}$$

where $H_n(X)$ are the Hermite polynomials, we can rewrite the initial state in the Fock space as

$$|\psi_0\rangle = \sum_n c_n |n\rangle |s\rangle, \qquad \text{(D3)}$$

with $c_n = \mathcal{N} \pi^{-1/4} \int dX \, \exp(-X^2/2) \langle n|X\rangle$. Hence the average position

$$\langle x \rangle = \langle \psi_0 | U^\dagger \hat{x} U | \psi_0 \rangle \qquad \text{(D4)}$$

and the corresponding variance

$$\Delta x = (\langle \psi_0 | U^\dagger \hat{x}^2 U | \psi_0 \rangle - \langle \psi_0 | U^\dagger \hat{x} U | \psi_0 \rangle^2)^{1/2} \qquad \text{(D5)}$$

can be obtained with respect to the time-evolved state $U(t)|\psi_0\rangle$ in a truncated Fock space with the maximum excitation number $n_{\max} = 512$. We remark that this truncation is verified to guarantee converging results, which are shown in Fig. 2 and Figs. 3(a) and 3(b) in the main text. In addition, the probability distribution of the wave packet $|\phi_f(x)|^2$ corresponding to the final state can be obtained by

$$|\phi_f(x)|^2 = \text{Tr}(\rho_x |x\rangle \langle x|) = \text{Tr}\left(\rho_x \sum_{n,n'} |n\rangle \langle n|x\rangle \langle x|n'\rangle \langle n'| \right), \qquad \text{(D6)}$$

where ρ_x is the reduced density matrix for the spatial degrees of freedom by tracing out the spin degree of freedom in the total final density matrix of the final state $U(t)|\psi_0\rangle \langle \psi_0 | U^\dagger(t)$.

[1] P. C. W. Davies, Quantum field theory in curved space–time, Nature (London) **263**, 377 (1976).

[2] T. Jacobson, Introduction to quantum fields in curved space-time and the Hawking effect, in *Lectures on Quantum Gravity* (Springer, Berlin, 2005), pp. 39–89.

[3] S. Hollands and R. M. Wald, Quantum fields in curved space-time, Phys. Rep. **574**, 1 (2015).

[4] R. Howl, L. Hackermülller, D. E. Bruschi, and I. Fuentes, Gravity in the quantum lab, Adv. Phys.: X **3**, 1383184 (2018).

[5] R. Howl, V. Vedral, D. Naik, M. Christodoulou, C. Rovelli, and A. Iyer, Non-gaussianity as a signature of a quantum theory of gravity, PRX Quantum **2**, 010325 (2021).

[6] W. G. Unruh, Experimental Black-Hole Evaporation?, Phys. Rev. Lett. **46**, 1351 (1981).

[7] S. Weinfurtner, E. W. Tedford, M. C. J. Penrice, W. G. Unruh, and G. A. Lawrence, Measurement of Stimulated Hawking Emission in an Analogue System, Phys. Rev. Lett. **106**, 021302 (2011).

[8] W. H. Zurek, Cosmological experiments in superfluid helium?, Nature (London) **317**, 505 (1985).

[9] P. O. Fedichev and U. R. Fischer, "Cosmological" quasiparticle production in harmonically trapped superfluid gases, Phys. Rev. A **69**, 033602 (2004).

[10] L. J. Garay, J. R. Anglin, J. I. Cirac, and P. Zoller, Sonic Analog of Gravitational Black Holes in Bose-Einstein Condensates, Phys. Rev. Lett. **85**, 4643 (2000).

[11] C. Barceló, S. Liberati, and M. Visser, Probing semiclassical analog gravity in Bose-Einstein condensates with widely tunable interactions, Phys. Rev. A **68**, 053613 (2003).

[12] P. O. Fedichev and U. R. Fischer, Gibbons-Hawking Effect in the Sonic de Sitter Space-Time of an Expanding Bose-Einstein-Condensed Gas, Phys. Rev. Lett. **91**, 240407 (2003).

[13] U. R. Fischer and R. Schützhold, Quantum simulation of cosmic inflation in two-component Bose-Einstein condensates, Phys. Rev. A **70**, 063615 (2004).

[14] I. Carusotto, S. Fagnocchi, A. Recati, R. Balbinot, and A. Fabbri, Numerical observation of Hawking radiation from acoustic black holes in atomic Bose–Einstein condensates, New J. Phys. **10**, 103001 (2008).

[15] J. Steinhauer, Observation of self-amplifying Hawking radiation in an analogue black-hole laser, Nat. Phys. **10**, 864 (2014).

[16] J. Steinhauer, Observation of quantum Hawking radiation and its entanglement in an analogue black hole, Nat. Phys. **12**, 959 (2016).

[17] S.-Y. Chä and U. R. Fischer, Probing the Scale Invariance of the Inflationary Power Spectrum in Expanding Quasi-Two-Dimensional Dipolar Condensates, Phys. Rev. Lett. **118**, 130404 (2017).

[18] J. R. M. De Nova, K. Golubkov, V. I. Kolobov, and J. Steinhauer, Observation of thermal Hawking radiation and its temperature in an analogue black hole, Nature (London) **569**, 688 (2019).

[19] M. Isoard and N. Pavloff, Departing from Thermality of Analogue Hawking Radiation in a Bose-Einstein Condensate, Phys. Rev. Lett. **124**, 060401 (2020).

[20] F. Belgiorno, S. L. Cacciatori, M. Clerici, V. Gorini, G. Ortenzi, L. Rizzi, E. Rubino, V. G. Sala, and D. Faccio, Hawking Radiation from Ultrashort Laser Pulse Filaments, Phys. Rev. Lett. **105**, 203901 (2010).

[21] T. G. Philbin, C. Kuklewicz, S. Robertson, S. Hill, F. König, and U. Leonhardt, Fiber-optical analog of the event horizon, Science **319**, 1367 (2008).

[22] J. Drori, Y. Rosenberg, D. Bermudez, Y. Silberberg, and U. Leonhardt, Observation of Stimulated Hawking Radiation in an Optical Analogue, Phys. Rev. Lett. **122**, 010404 (2019).

[23] S. Lang and R. Schützhold, Analog of cosmological particle creation in electromagnetic waveguides, Phys. Rev. D **100**, 065003 (2019).

[24] D. Boiron, A. Fabbri, P.-E. Larré, N. Pavloff, C. I. Westbrook, and P. Ziń, Quantum Signature of Analog Hawking Radiation in Momentum Space, Phys. Rev. Lett. **115**, 025301 (2015).

[25] A. Roldán-Molina, A. S. Nunez, and R. A. Duine, Magnonic Black Holes, Phys. Rev. Lett. **118**, 061301 (2017).

[26] I. Chuang, R. Durrer, N. Turok, and B. Yurke, Cosmology in the laboratory: Defect dynamics in liquid crystals, Science **251**, 1336 (1991).

[27] C. Barceló, S. Liberati, and M. Visser, Analogue gravity, Living Rev. Relativ. **14**, 3 (2011).

[28] D. Faccio, F. Belgiorno, S. Cacciatori, V. Gorini, S. Liberati, and U. Moschella, *Analogue Gravity Phenomenology: Analogue Spacetimes and Horizons, From Theory to Experiment* (Springer, Berlin, 2013), Vol. 870.

[29] P. M. Alsing, J. P. Dowling, and G. J. Milburn, Ion Trap Simulations of Quantum Fields in an Expanding Universe, Phys. Rev. Lett. **94**, 220401 (2005).

[30] R. Schützhold, M. Uhlmann, L. Petersen, H. Schmitz, A. Friedenauer, and T. Schätz, Analogue of Cosmological Particle Creation in an Ion Trap, Phys. Rev. Lett. **99**, 201301 (2007).

[31] N. C. Menicucci, S. J. Olson, and G. J. Milburn, Simulating quantum effects of cosmological expansion using a static ion trap, New J. Phys. **12**, 095019 (2010).

[32] J. Casanova, J. J. García-Ripoll, R. Gerritsma, C. F. Roos, and E. Solano, Klein tunneling and Dirac potentials in trapped ions, Phys. Rev. A **82**, 020101(R) (2010).

[33] R. Gerritsma, B. P. Lanyon, G. Kirchmair, F. Zähringer, C. Hempel, J. Casanova, J. J. García-Ripoll, E. Solano, R. Blatt, and C. F. Roos, Quantum Simulation of the Klein Paradox with Trapped Ions, Phys. Rev. Lett. **106**, 060503 (2011).

[34] M. Wittemer, F. Hakelberg, P. Kiefer, J.-P. Schröder, C. Fey, R. Schützhold, U. Warring, and T. Schaetz, Phonon Pair Creation by Inflating Quantum Fluctuations in an Ion Trap, Phys. Rev. Lett. **123**, 180502 (2019).

[35] Z. Tian, Y. Lin, U. R. Fischer, and J. Du, Verifying the upper bound on the speed of scrambling with the analogue Hawking radiation of trapped ions, Eur. Phys. J. C **82**, 212 (2022).

[36] R.-Q. Yang, H. Liu, S. Zhu, L. Luo, and R.-G. Cai, Simulating quantum field theory in curved spacetime with quantum many-body systems, Phys. Rev. Research **2**, 023107 (2020).

[37] P. D. Nation, M. P. Blencowe, A. J. Rimberg, and E. Buks, Analogue Hawking Radiation in a dc-SQUID Array Transmission Line, Phys. Rev. Lett. **103**, 087004 (2009).

[38] C. Sabín, Quantum simulation of traversable wormhole spacetimes in a dc-SQUID array, Phys. Rev. D **94**, 081501(R) (2016).

[39] Z. Tian, J. Jing, and A. Dragan, Analog cosmological particle generation in a superconducting circuit, Phys. Rev. D **95**, 125003 (2017).

[40] Z. Tian and J. Du, Analogue Hawking radiation and quantum soliton evaporation in a superconducting circuit, Eur. Phys. J. C **79**, 994 (2019).

[41] P. Collas and D. Klein, *The Dirac Equation in Curved Spacetime* (Springer International Publishing, Berlin, 2019).

[42] J. S. Pedernales, M. Beau, S. M. Pittman, I. L. Egusquiza, L. Lamata, E. Solano, and A. del Campo, Dirac Equation in $(1 + 1)$-Dimensional Curved Spacetime and the Multiphoton Quantum Rabi Model, Phys. Rev. Lett. **120**, 160403 (2018).

[43] J. F. García and C. Sabín, Dirac equation in exotic spacetimes, Phys. Rev. D **99**, 025008 (2019).

[44] L. Lamata, J. León, T. Schätz, and E. Solano, Dirac Equation and Quantum Relativistic Effects in a Single Trapped Ion, Phys. Rev. Lett. **98**, 253005 (2007).

[45] M. Alcubierre, The warp drive: Hyper-fast travel within general relativity, Class. Quantum Grav. **11**, L73 (1994).

[46] S. Finazzi, S. Liberati, and C. Barceló, Semiclassical instability of dynamical warp drives, Phys. Rev. D **79**, 124017 (2009).

[47] H. White, A discussion of space-time metric engineering, Gen. Relativ. Gravit. **35**, 2025 (2003).

[48] H. White, Warp field mechanics 101, in *DARPA/NASA 100 Year Starship Symposium*, Report No. JSC-CN-24651 (2011).

[49] E.-A. Kontou and K. Sanders, Energy conditions in general relativity and quantum field theory, Class. Quantum Grav. **37**, 193001 (2020).

[50] E. Curiel, A primer on energy conditions, in *Towards a Theory of Spacetime Theories*, edited by D. Lehmkuhl, G. Schiemann, and E. Scholz (Springer, New York, 2017), pp. 43–104.

[51] K. D. Olum, Superluminal Travel Requires Negative Energies, Phys. Rev. Lett. **81**, 3567 (1998).

[52] C. Barcelo and M. Visser, Twilight for the energy conditions?, Int. J. Mod. Phys. D **11**, 1553 (2002).

[53] U. R. Fischer and M. Visser, Warped space-time for phonons moving in a perfect nonrelativistic fluid, Europhys. Lett. **62**, 1 (2003).

[54] P. F. González-Díaz, Warp drive space-time, Phys. Rev. D **62**, 044005 (2000).

[55] R. B. Mann, S. M. Morsink, A. E. Sikkema, and T. G. Steele, Semiclassical gravity in 1+1 dimensions, Phys. Rev. D **43**, 3948 (1991).

[56] B. Thaller, *The Dirac Equation* (Springer Science & Business Media, Berlin, 2013).

[57] S. C. Burd, R. Srinivas, H. M. Knaack, W. Ge, A. C. Wilson, D. J. Wineland, D. Leibfried, J. J. Bollinger, D. T. C. Allcock, and D. H. Slichter, Quantum amplification of boson-mediated interactions, Nat. Phys. **17**, 898 (2021).

[58] S. C. Burd, R. Srinivas, J. J. Bollinger, A. C. Wilson, D. J. Wineland, D. Leibfried, D. H. Slichter, and D. T. C. Allcock, Quantum amplification of mechanical oscillator motion, Science **364**, 1163 (2019).

[59] A. Sørensen and K. Mølmer, Quantum Computation with Ions in Thermal Motion, Phys. Rev. Lett. **82**, 1971 (1999).

[60] R. Srinivas, S. C. Burd, R. T. Sutherland, A. C. Wilson, D. J. Wineland, D. Leibfried, D. T. C. Allcock, and D. H. Slichter, Trapped-Ion Spin-Motion Coupling with Microwaves and a Near-Motional Oscillating Magnetic Field Gradient, Phys. Rev. Lett. **122**, 163201 (2019).

[61] G. E. Volovik, *The Universe in a Helium Droplet* (Oxford University Press on Demand, Oxford, 2003), Vol. 117.

[62] G. E. Volovik, Black hole and Hawking radiation by type-II Weyl fermions, JETP Lett. **104**, 645 (2016).

[63] J. Nissinen and G. E. Volovik, Type-III and IV interacting Weyl points, JETP Lett. **105**, 447 (2017).

[64] A. Weststrom and T. Ojanen, Designer Curved-Space Geometry for Relativistic Fermions in Weyl Metamaterials, Phys. Rev. X **7**, 041026 (2017).

[65] L. Liang and T. Ojanen, Curved spacetime theory of inhomogeneous Weyl materials, Phys. Rev. Research **1**, 032006(R) (2019).

[66] T. Farajollahpour, Z. Faraei, and S. A. Jafari, Solid-state platform for space-time engineering: The 8*Pmmn* borophene sheet, Phys. Rev. B **99**, 235150 (2019).

[67] T. Farajollahpour and S. A. Jafari, Synthetic non-Abelian gauge fields and gravitomagnetic effects in tilted Dirac cone systems, Phys. Rev. Research **2**, 023410 (2020).